

Ubiquity of chaotic magnetic-field lines generated by three-dimensionally crossed wires in modern electric circuits

M. Hosoda,¹ T. Miyaguchi,¹ K. Imagawa,¹ and K. Nakamura^{1,2}

¹*Department of Applied Physics, Osaka City University, Sugimoto, Sumiyoshi-ku, Osaka 558-8585, Japan*

²*Heat Physics Department, Uzbek Academy of Sciences, 28 Kataltal Street, 100135 Tashkent, Uzbekistan*

(Received 17 July 2009; revised manuscript received 19 October 2009; published 21 December 2009)

We investigate simple three-dimensionally crossed wires carrying electric currents which generate chaotic magnetic-field lines (CMFLs). As such wire systems, cross-ring and perturbed parallel-ring wires are studied, since topologically equivalent configurations to these systems can often be found in contemporary electric and integrated circuits. For realistic fundamental wire configurations, the conditions for wire dimensions (size) and current values to generate CMFLs are numerically explored under the presence of the weak but inevitable geomagnetic field. As a result, it is concluded that CMFLs can exist everywhere; i.e., they are ubiquitous in the modern technological world.

DOI: [10.1103/PhysRevE.80.067202](https://doi.org/10.1103/PhysRevE.80.067202)

PACS number(s): 05.45.-a, 03.50.De, 41.20.Gz

It is commonly believed that the magnetic-field lines (MFLs) generated by a wire carrying electric current always have simple closed-loop structures such as the examples cited in many textbooks [1,2]. However, this belief is wrong because chaotic magnetic-field lines (CMFLs) may emerge from simple as well as complex wire configurations as pointed out by Ulam [3]. While CMFLs in coil or ring currents were well investigated in the context of plasma confinement for nuclear fusion [4–7], most of unperturbed systems in the theoretical treatment were limited to straight plasma currents, diverter currents, unbent (straight) helical currents, and their combinations and no investigations were made on cross-ring, parallel-ring wires and other topologically equivalent configurations as unperturbed systems. Although recent works [8–10] numerically showed that a rippled ring wire can produce CMFLs, the proposed wire configurations were rather complex. Furthermore, there has been no report on the likelihood of CMFLs emerging from actual electrical and electronic devices in our daily life.

Here, with the use of several simple wire configurations, we show behaviors of the CMFL generation, which comes from homoclinic intersections near an unstable fixed point [6,11–16]. We also investigate other topologically equivalent simple wire configurations which are encountered in realistic electric and electronic circuits with taking account of the inevitable geomagnetic field (GF) in the real world, and then we reveal general existence of the CMFL in these systems.

In the analysis of systems in Figs. 1 and 2, we assume the zero-GF condition in which we use a unity current. For the other systems, we apply GF and use realistic current values. The used currents are equivalent for all wires in a given system. The three-dimensional simulations of the magnetic-field lines for simple configurations such as straight and ring wires are performed by using analytical expressions of magnetic fields [2]. For some finite-length wires for which we cannot derive analytical forms of the magnetic fields, we use the Biot-Savart law for numerical integrations.

Figure 1 shows the simplest two-wire system which generates CMFLs. The system is composed of two perpendicularly crossed rings of the same radius a with their centers also separated by a . For this system, the analytic expression

of the magnetic field can be easily derived by a superposition of the complete elliptic integrals [2], and we have used this explicit expression (not shown) for numerical integrations. As shown in Fig. 1(a), when an MFL starts from a certain area, it has a complex trajectory. The trajectory changes drastically with a slight deviation of the initial coordinates of the MFL. This is a well-known property of chaotic orbits. Figures 1(b) and 1(c) show the Poincaré map and Lyapunov exponent of the CMFL, respectively. The collapse of tori in the Poincaré surface of section and the positive value of Lyapunov exponent imply that the MFL is chaotic [11,14], i.e., CMFL.

To overview the behavior of the CMFLs, we tracked the development of the trajectory. Figure 1(a) shows the progressive sequence of a CMFL. The MFL first starts from the position 1, twines the A-ring (1–3), travels around the ring and returns back to the central area (4), changes its twine to the B-ring (5–8), and then irregularly repeats the alternation of the wrapping ring, i.e., sequences (8–16) for A-ring, (16–20) for B-ring, and (20–28) for A-ring. This sort of behavior is well known as the itinerancy of the orbit in chaos theory, which is also observed in the restricted three-body problem studied by Poincaré as the complex orbit of a planet traveling around a binary star [15,16]. One of the generation mechanisms of CMFLs in this system is considered to be the homoclinic intersections around unstable fixed points, which are created by perturbed parallel current-carrying rings shown in Fig. 2. Although the detailed analysis has already been reported in the context of plasma physics [6,17,18], we restate the phenomenon of the homoclinic intersections briefly by using a simple wire model in the following paragraph:

To begin with, we consider a single-coil system in Fig. 2(a). Its rotational symmetry around the Z axis makes it possible to decompose the system into a one-degree-of-freedom Hamiltonian system with an extra independent variable [4–7]:

$$\dot{q} = \frac{\partial H}{\partial p}(q,p), \quad \dot{p} = -\frac{\partial H}{\partial q}(q,p), \quad \dot{\phi} = 0, \quad (1)$$

where the canonical variables q and p are related to the cylindrical coordinates (r, ϕ, z) as $q=z$ and $p=r^2$, respectively.

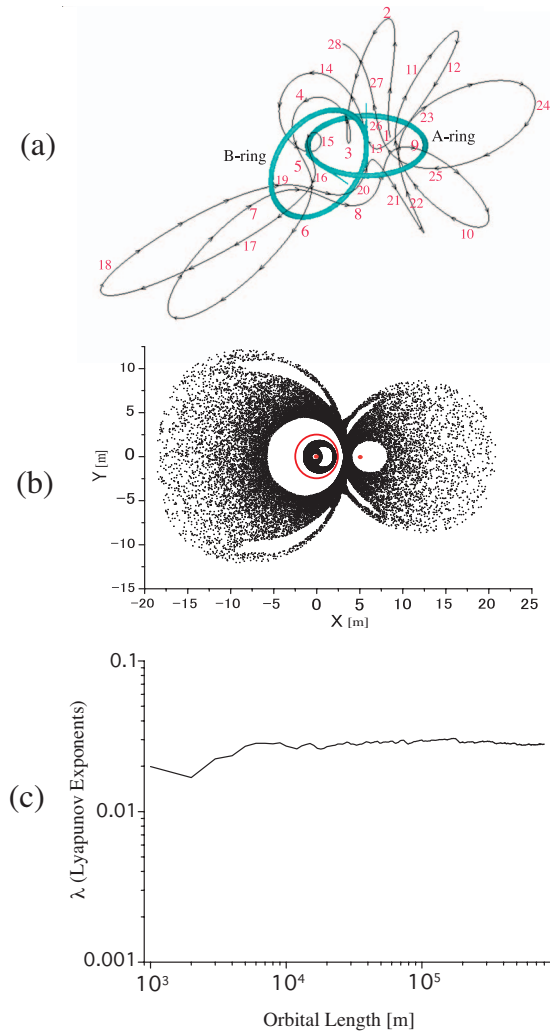


FIG. 1. (Color) (a) Perpendicularly crossed ring structure (blue), a CMFL (black), and progression of a CMFL (red numbers). [(b) and (c)] Poincaré map (b) and Lyapunov exponent (c) of a CMFL in the cross-ring system ($a=2.5$ m). The cross-section plane of the Poincaré map is the X - Y plane and the axis unit is meter. The red circle and two red dots indicate the positions of the ring wires. The horizontal axis in (c) is orbital length of the CMFL with calculation steps of 10^{-5} m.

The Hamiltonian $H(q,p)$ is given by $H(q,p)=2rA_\phi$, where A_ϕ is the ϕ component of the vector potential [2]. This kind of decomposition into an integrable Hamiltonian system and a noncanonical variable is always possible for three-dimensional ordinary differential equations with divergence-free vector fields, e.g., incompressible fluid flows and magnetic fields, if the system has a continuous symmetry [12]. The one-degree-of-freedom systems are integrable and, hence, there is no CMFL. As shown in Fig. 2(a), the phase space of this system forms a single nested structure of MFLs (torus). By contrast, when another coil is placed as displayed in Fig. 2(b), the phase-space structures change qualitatively. Here, the second coil is parallel to the X - Y plane and its center is located on the Z axis. Again, a reduction to an integrable Hamiltonian system is possible thanks to the rotational symmetry and, in the phase space of this reduced sys-

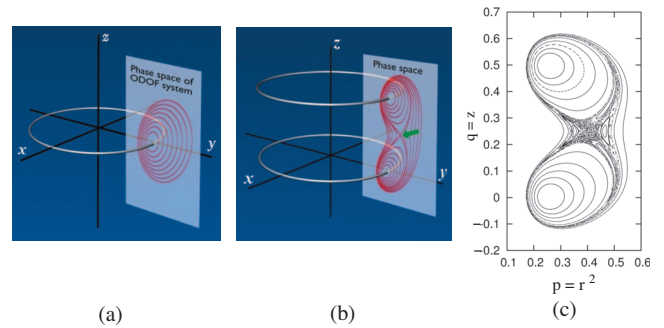


FIG. 2. (Color) (a) Single-ring coil system (silver) and its phase space (red curves). (b) A system composed of two parallel rings (silver) and its phase space (red curves). The green arrow indicates the unstable fixed point. (c) Poincaré surface of the parallel-ring system with a straight wire on the Z axis perturbed by a uniform magnetic field along the X axis.

tem, there is a separatrix and an unstable fixed point [13,14] as shown in Fig. 2(b). Moreover, in order to ensure the non-resonant condition, we placed a straight wire on the Z axis, which changes the equation for ϕ into $\dot{\phi}=\Omega(p)$ with a function $\Omega(p)$ but does not alter the Hamiltonian $H(q,p)$. Consequently, the breaking of symmetry due to small perturbations can generate chaos through the mechanism known as homoclinic intersections [6,11–14] as shown in Fig. 2(c), where the system is subjected to a weak uniform magnetic field. In general, the type of perturbation is not important for the generation of chaos as long as it can break the rotational symmetry.

Hereafter, we present more realistic wire configurations under a weak but nonzero GF. Figure 3(a) shows a system of mutually perpendicular separated rings. Figures 3(b) and 3(c) show a CMFL in the system and a Poincaré map. Figure 3(d) shows the vanishing of CMFL under a weak wire-current condition. Since the magnetic field is composed of a weak magnetic field from the wire and a relatively stronger GF, the MFL is dominantly pulled or washed out by the GF and escapes to infinity. We should note that this escaping behavior is interpreted as an example of chaotic scattering [6]. This suggests that the observation of CMFL in small systems with weak current intensity is difficult and this fact was also overlooked in Refs. [9,10]. In fact, many systems composed of single-wire coils need greater than 10^4 A current to overcome the GF in our simulation for the 5-cm-diameter coils in Fig. 1. By contrast, the separate-ring system is optimum for experimental verification of CMFL, because the rings can be composed of multiturn coils so as to generate a strong magnetic field that overcomes the GF flow. In other words, for example, 100 A current in a single wire can be replaced by 1 A in the 100-turn coils in Fig. 3. We should also note that it is difficult to make multiturn coils in the cross-ring system in Fig. 1.

Under the ideal conditions, i.e., zero or small GF, CMFLs can localize in a bounded region and fill it everywhere densely. This is due to the barriers of the torus surrounding CMFLs [for example, see Fig. 2(c)]. In general, however, CMFLs drift due to the effect of GF and gradually escape to infinity as shown in Fig. 3(d). This unboundness of MFLs

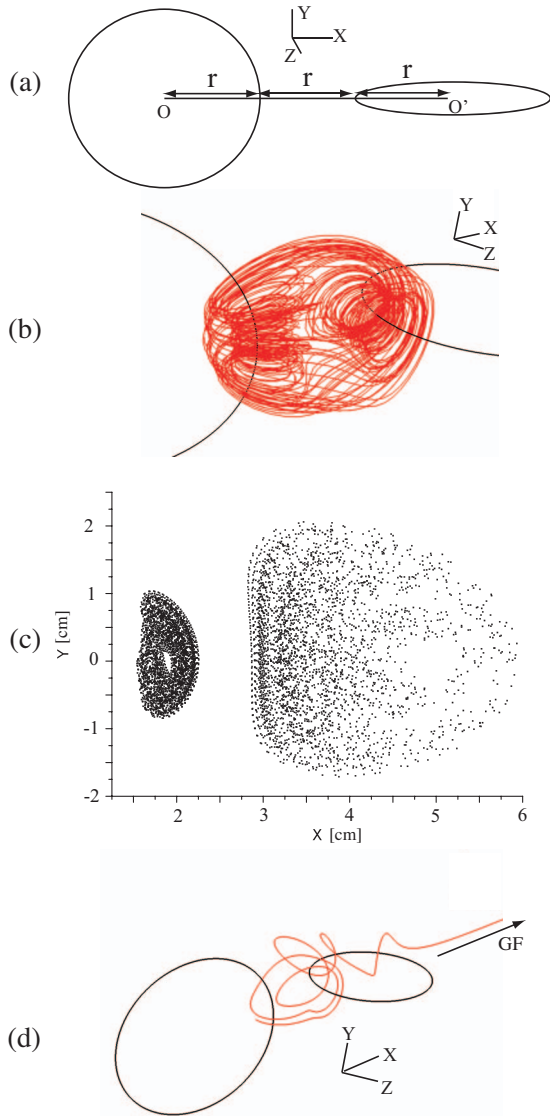


FIG. 3. (Color) (a) Separated perpendicular rings. Ring radius r , their separation, and the current value are 2.5 cm, 2.5 cm, and 100 A, respectively. The center coordinates of the rings are (0, 0, 0) and (7.5, 0, 0) in units of centimeters. [(b) and (c)] Generated CMFL (b) (red curves) and a Poincaré map (c) at the X - Y plane under 0.5 G GF along the X axis. (d) Vanishing of the CMFL (red) due to washing out of the MFL by the GF under a weak wire-current condition (10 A). The GF direction is along the X axis. The calculation methods are equivalent to those in Fig. 1.

can be understood as transient chaos. In spite of this transience of CMFLs under GF, however, MFLs still have complex structures and temporally exhibit a chaotic nature as indicated by the Poincaré surfaces. This transient chaos persists for long, when the wire separation is close and the current is sufficiently large.

Next, we proceed to study a variety of realistic wire configurations in conventional electrical products under the GF and examine the possible existence of CMFL there. Some of these wire configurations have a topology similar to the above-mentioned systems. Figure 4 shows some realistic examples of generating a CMFL in our simulation with realistic dimensions (size and separation) and current values under

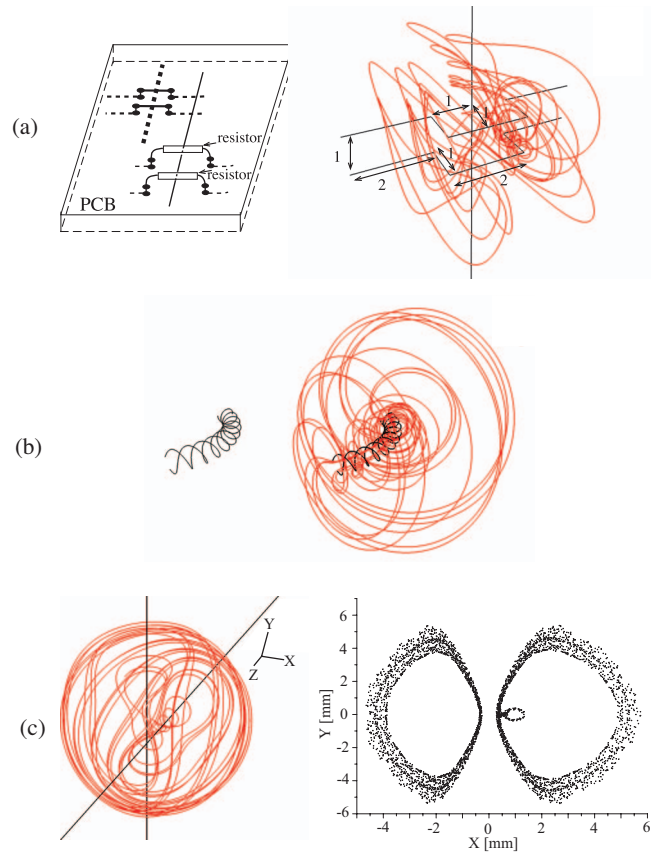


FIG. 4. (Color) (a) Schematic figure of a realistic system, which corresponds to circuits on two-layer PCBs or a multilayer interconnection in ICs. The solid and dashed lines indicate wires deposited on the front and back surfaces of the PCB, respectively. Right figure of (a): a generated CMFL. The wire dimensions are indicated by the numbers near the arrowed lines in millimeter and micrometer units for PCB and IC, respectively. The current and the vertical separation of the wires are 1 A and 1 mm for PCB and 1 mA and 1 μm for IC, respectively. (b) Schematic figure of a curved twisted-pair wire (black) and its CMFL (red) (right figure). The separation of the wires and the current value are 2 mm and 20 A. (c) Two separated cross wires (black) and their CMFL (red), and its Poincaré map at the X - Y plane (right figure). The wires do not contact each other but are separated slightly at the crossing point (0, 0, 0) toward the X direction of the figure. The wire separation and current are 1 mm and 1 A for PCBs, which are values equivalent to 1 μm and 1 mA for ICs. The normalized GF vector components are $(0, \sqrt{1/2}, \sqrt{1/2})$.

0.5 G GF; such sub-Gauss GF is typical in many countries.

Figure 4(a) shows systems composed of two rectangular wires and a normal straight wire and a generated CMFL (right figure). The system has similar topology to that in Fig. 2, since the rectangles correspond to the rings and the symmetry is broken (half circle rings). This wire configuration is frequently used to cross different lines in multilayer printed circuit boards (PCBs) and multilayer integrated circuits (ICs). We note that the electric resistors in Fig. 4(a) are equivalent to wires, since current flows through them. We also note that the smaller the separation of the wires, the smaller the necessary current intensity to overcome the GF effect. This comes from the scaling law of magnetic-field equations. For example, regarding the separate-rings system

in Fig. 3, when the coil diameter is reduced to $50\ \mu\text{m}$, i.e., 10^{-3} times 5 cm, the necessary current is reduced to 1 A ($10^3\ \text{A} \times 10^{-3}$). Since the separation of wires on two layers (for example, front and back surfaces of PCBs) is very short, i.e., on the order of 1 mm for PCBs and $1\ \mu\text{m}$ or much less for ICs, the necessary current to generate a CMFL under the GF can be small. For example, currents greater than or equal to 1 A frequently exist on 1-mm-thick PCBs of power regulators in common personal computers and digital home electronics, and several tens of amperes are frequent for a 3 V power supply used by modern desktop personal computers. Moreover, in modern power electronics, switching regulators are common and their instantaneous currents may exceed 10 A with thin pattern widths on PCBs. For ICs, 1 mA current is sufficient to cause CMFLs, which is also possible as continuous current in many power ICs or surge currents for digital signal transmission in many high-speed ICs. Therefore, the system in Fig. 4(a) is realistic and, thus, CMFLs can be generated in many modern electric and electronic products.

Figure 4(b) shows a CMFL generated by a curved twisted-pair cable, which is frequently encountered in some power supply cables (power wires), as well as local area network cables and universal serial bus cables. This twisted-pair system might be interpreted as a consecutive topological extension of the breaking cross-ring system. For power wires in modern personal computers, currents of several tens of amperes are frequent with separation of only a few millimeters. This condition might also be seen in household wiring for ac power supply. We should note that this might also be the case for parallel-wire cables, which are occasionally twisted and curved. Consequently, it is possible that CMFL exists everywhere in our lives.

The system in Fig. 4(c), which is composed of two sepa-

rated straight wires, has an interesting feature: the system shows no CMFL under zero GF. The chaos in this system only emerges with the assistance of the GF. The two wires are crossed but slightly separated from each other; for example, one wire is on the Z axis and the other is parallel to the Y axis but slightly away from the YZ plane. From our numerical simulation, this system has a separatrix [cf. Fig. 2(b)]. Therefore, a perturbation by the GF can generate CMFLs. Without GF, each MFL forms a spiral along the wires and tends to escape from the central crossing area to infinity. Therefore, from another viewpoint, GF plays the role of rolling back these MFLs to the central area. The needed direction of the North or South Pole to generate CMFL was about 45° to the wires, and we found from our simulation that the tolerance of the angle for the CMFL generation was about 30° in all three-dimensional directions. Therefore, conventional electric circuits with a similar configuration, for example, double-layer PCBs having a wire on the front layer and another on the back layer, can generate CMFLs with the help of the GF when the circuits in the PCB face in the proper direction robustly. Since the relevant dimensions (size) and currents are typical values in the modern technological world, the chaos in this system arises occasionally and is also ubiquitous depending on the direction of electrical and electronic products (e.g., portable computers, ICs in cell phones, and car electronics) toward the North Pole.

In summary, we showed CMFLs emerging from some simple current-carrying wire configurations. We also revealed the existence of CMFLs in a variety of realistic wire configurations under the GF, and thus, it is concluded that the CMFL is ubiquitous in the modern technological world.

K.N. is grateful for the support received through a project of the Uzbek Academy of Sciences (Grant No. FA-F2-084).

-
- [1] D. J. Griffiths, *Introduction to Electrodynamics* (Prentice-Hall International, New Jersey, 1999), Chap. 5.
- [2] L. D. Landau, L. P. Pitevskii, and E. M. Lifshitz, *Electrodynamics of Continuous Media*, 2nd ed. (Elsevier, Oxford, 1984), Chap. 30.
- [3] S. M. Ulam, *A Collection of Mathematical Problems* (Interscience Publishers, New York, 1960), Chap. 7, pp. 107–108; S. M. Ulam, republished as *Problems in Modern Mathematics* (Dover Publications, New York, 2004).
- [4] V. K. Mel'nikov, *Sov. Phys. Dokl.* **7**, 502 (1962).
- [5] J. R. Cary and R. G. Littlejohn, *Ann. Phys.* **151**, 1 (1983).
- [6] S. S. Abdullaev, *Construction of Mappings for Hamiltonian Systems and Their Applications* (Springer-Verlag, Berlin, 2006).
- [7] A. H. Boozer, *Rev. Mod. Phys.* **76**, 1071 (2005).
- [8] P. J. Morrison, *Phys. Plasmas* **7**, 2279 (2000).
- [9] J. Aguirre and D. Peralta-Salas, *Europhys. Lett.* **80**, 60007 (2007).
- [10] J. Aguirre, J. Giné, and D. Peralta-Salas, *Nonlinearity* **21**, 51 (2008).
- [11] G. M. Zaslavsky, *Hamiltonian Chaos & Fractional Dynamics* (Oxford University Press, New York, 2005), Chaps. 2 and 23.
- [12] I. Mezić and S. Wiggins, *J. Nonlinear Sci.* **4**, 157 (1994).
- [13] J. Guckenheimer and P. Holmes, *Nonlinear Oscillations, Dynamical Systems, and Bifurcations of Vector Fields* (Springer-Verlag, New York, 1997).
- [14] A. J. Lichtenberg and M. A. Leiberman, *Regular and Chaotic Dynamics*, 2nd ed. (Springer-Verlag, New York, 1992).
- [15] F. Diacu and P. Holmes, *Celestial Encounters: The Origins of Chaos and Stability* (Princeton University Press, Princeton, NJ, 1996).
- [16] H. Poincaré, *New Methods of Celestial Mechanics* (American Institute of Physics, New York, 1992).
- [17] Y. Tomita, S. Seki, and H. Momota, *J. Phys. Soc. Jpn.* **42**, 687 (1977).
- [18] Y. Tomita, Y. Nomura, H. Momota, and R. Itatani, *J. Phys. Soc. Jpn.* **44**, 637 (1978).